A LOW COST MODEL AIRCRAFT FLIGHT RESEARCH FACILITY IN WIND TUNNEL

Bowen NIE[*], Linliang GUO[†], Fei CEN[†], Olivier SENAME[‡], Luc DUGARD[‡]
*** College of Intelligence Science and Engineering, National University of Defense Technology, Changsha 410073, China**
† Low Speed Aeronautics Institution, China Aerodynamics Research and Development Center, Mianyang 621000, China
‡ Univ. Grenoble Alpes, CNRS, Grenoble INP[§], GIPSA-lab, 38000 Grenoble, France
[§] Institute of Engineering, Univ. Grenoble Alpes
Keywords: *wind tunnel, virtual flight test, dynamic scaling, flight control law*

Abstract

This paper presents the overview of a low cost, generic aircraft model flight research facility housed in a wind tunnel at the Low Speed Aeronautics Institution (LSAI) of China Aerodynamics Research and Development Center (CARDC). It offers a cost effective way to investigating flight dynamics and evaluating designed control laws. First, the purpose and characteristics of the facility are described, alongside the description of the 3-DOF maneuver rig, dynamically scaled design and avionic system. The effectiveness of the proposed low-cost experimental facility is demonstrated via simulations and the virtual flight test involving a sub-scaled aircraft model with a scenario of performing conventional maneuvers.

1 Introduction

Recently, significant research has been performed on the development of unsteady aerodynamics modeling[1,2], flight control in extended envelop[3,4] and upset conditions[5], self-repairing control in failure conditions[6], or flight testing of novel aircraft configurations[7]. However, flight test and validation with full-scale manned aircraft has been recognized as a significant challenge due to the cost, efficiency and risks in the early research phase of the advanced techniques. It is of practical interest to address these needs with flying tests in wind tunnel, since the sub-scaled models are much less expensive and the flight risks are largely relieved with the help of safety instrumentations. In addition, the test setups, including aircraft model configuration, wind tunnel flow field, structure and gains of flight control law, are economical in terms of cost and time when they are modified or repeated.

Several flying test techniques using wind tunnels have been developed over the past decades, as reviewed in [8, 9]. There are 3 most popular testing setups: 3-DOF, 4-DOF and 6-DOF. The 3-DOF setup allows the sub-scaled model to rotate aligning three body axes but restrains translation motion[10,11,12]. The most important attitude motion (pitch, roll and yaw) of aircraft model is physically simulated and the flying qualities and control law effects, up to large angle-of-attack, can be studied. The 4-DOF setup allows the flyable model to slide vertically in addition to three axes rotation[13,14]. The coupled motion, such as the combination of pitch and heave, can be performed in order to simulate the onset of dynamic behavior more realistically. In the 6-DOF setup, the model is held by the engine thrust and aerodynamic forces in the wind tunnel test section[15, 16]. Indeed, this is the ideal setup for flying tests in wind tunnel. However, it is necessary to equip the scaled aircraft model with engine for propulsion simulation and 3 pilots for manipulation and evaluation[17]. Obviously, the 6-DOF setup is much more complicated and expensive than the 3/4-DOF setup.

The flying test techniques in wind tunnels have proliferated in recent years in China due to the

need for validation and evaluation of flight control law, in particular for challenging flight regimes [18,19,20]. A low cost virtual flight test (VFT) facility was devised, which aims to support research activities within the LSAI including improved unsteady aerodynamics modeling and radical control law validation. This paper describes the facility and its features, including a 3-DOF rig for almost frictionless model support, subscale model for dynamic scaling, avionics for Rapid Control Prototyping (RCP) and some illustrative results. The results highlight the flight testing capability, flexibility and simplicity to validate flight control laws for aircrafts.

2 Model Aircraft Research Facility

The overview of the virtual flight test system is shown in Fig 1. A rig with a spherical rolling joint is employed to have the model move in response to the control and aerodynamics loads. The rig can provide a near frictionless pivot for the model in center of the wind tunnel. The model is unpowered, properly scaled down in mass and moments of inertia, as well as in dimensions, in order to provide dynamic stability and control results that are directly applicable to the corresponding full-scale airplane.

Fig. 1. Overview of the Model Aircraft Flight Research Facility

2.1 The 3-DOF Rig

Fig 2 presents the 3-DOF model support rig layout along with a spherical rolling joint. The vertical support holds the spherical rolling joint, which attaches to center-of-gravity (CG) of the aircraft model and allows for unlimited yaw and ±45° pitch/roll capability.

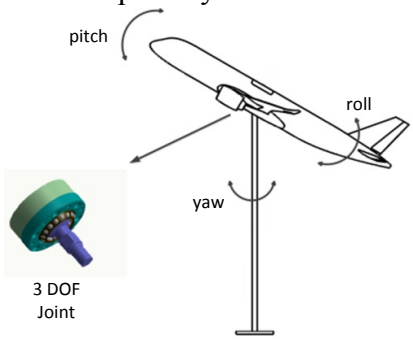

Fig. 2. The 3-DOF Rig and Spherical Rolling Joint

For the aircraft model dynamics, it is assumed that:

- The misalignment of aircraft model's CG to the center of joint is not taken into account.
- The effects of aerodynamic interference from the rig are not modeled.

The motion of the aircraft model can be represented by the following differential equations[19]:

$$\begin{cases} m(\dot{u}+qw-rv)=0 \\ m(\dot{v}+ru-pw)=0 \\ m(\dot{w}+pv-qu)=0 \\ I_x\dot{p}+(I_z-I_y)qr-I_{xz}(pq+\dot{r}) \\ +I_{yz}(r^2-q^2)+I_{xy}(pr+\dot{q})=L \\ I_y\dot{q}+(I_x-I_z)rp+I_{xz}(p^2-r^2) \\ +I_{yz}(pq-\dot{r})-I_{xy}(qr+\dot{p})=M \\ I_z\dot{r}+(I_y-I_x)pq+I_{xz}(qr-\dot{p}) \\ -I_{yz}(pr+\dot{q})+I_{xy}(q^2+p^2)=N \end{cases} \quad (1)$$

where m is the mass of aircraft model, I_x, I_y, I_z are the inertia of three axes respectively, I_{xz}, I_{yz}, I_{xy} are the cross inertia, u, v, w are the velocity components in body axis system, p, q, r are the roll rate, pitch rate and yaw rate respectively, and L, M, N are the moment components in body axis system. As a result, the external moments L, M and N acted on the aircraft model consist of the aerodynamic and joint friction moments.

In order to identify the coefficients of friction, oscillations on a set of spring suspension of each DOF of the aircraft model without flow are

tested, as shown in Fig 3. The angle and angle rate are measured by the onboard Attitude Heading Reference System (AHRS) and recorded by the data acquire system. Taking the pitch DOF as an example, the friction model could be approximated by a linear second-order transfer function.

$$I_y\ddot{\theta} + \text{sign}(\dot{\theta})M_f + 2kl^2\theta = 0 \qquad (2)$$

where θ is the pitch angel, k is the stiffness coefficient of spring, l is the distance from the connecting point of spring to the rotating center of joint, M_f is the moment due to friction.

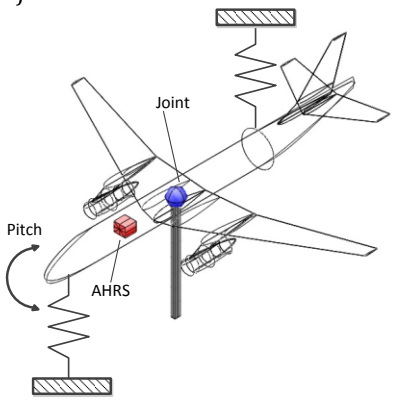

Fig. 3. Pitch Damping Test Setup

Estimates of the friction damping coefficient are then deduced from a curve fitting an exponentially-decaying sine waveform to the data[21]. Damping coefficients for pitch, yaw and roll have been identified and summarized in Table 1. The friction induced damping is less than 1% of the typical modal damping of aircrafts. One can see that the friction of the 3-DOF joint is small and does not affect significantly the aircraft model dynamics.

Table 1. Damping Parameters for 3-DOF Joint

	ξ	$\omega_n(\text{rad/s})$
pitch	0.0050	8.05
yaw	0.0026	7.66
roll	0.0060	24.16

2.2 Subscale Model

As previously mentioned, the aircraft model needs to be dynamically scaled by matching of the dynamic parameters, as summarized in Table 2. The models are Froude scaled to provide Froude number similitude and thus assure similitude of inertial and gravitational effects during the maneuvers and the flights in steady-state. As a result, the aircraft model should not only be scaled dimensionally, but also in weight, inertias, control, and actuation systems[8,22].

Table 2. Dynamic scaling parameters for Froude philosophy

Parameter	Scale factor
Linear dimension	N
Relative density	1
Froude number	1
Weight, mass	N^3
Moment of inertia	N^5
Linear velocity	$N^{0.5}$
Linear acceleration	1
Angular velocity	$N^{-0.5}$
Angular acceleration	N^{-1}
Time	$N^{0.5}$
Reynolds number	$N^{1.5}$
Dynamic pressure	N

The models tested are normally constructed of aluminum framework and carbon fiber skin to withstand the payload and to reduce the weight of airframe as much as possible. The maximum model's wing span is limited to be not more than 2/3 of the width of the wind tunnel. The normal geometric scales are about 1/10 of the typical full-scale airplanes, which results in models with lengths of about 2 meters, wingspans of 1.5 to 2 meters, and weights of 20 to 30 kilograms.

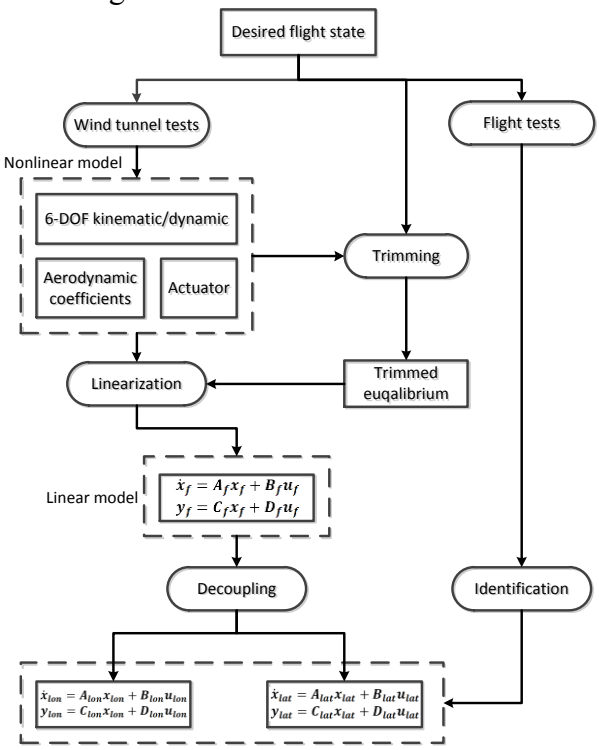

Fig. 4. Procedures for modeling of scaled aircraft

Mathematical model of scaled aircraft is required for dynamic characteristics analysis and control law synthesis. The decoupled linear model can be extracted from the nonlinear flight dynamic model or identified from flight test data, as shown in Fig 4. The nonlinear model is built with the aerodynamic coefficients from wind tunnel tests, including static stability derivatives, control effectiveness, and dynamic stability derivatives.

2.3 Avionic System

To achieve the flight control research objectives, the avionic instrumentation is designed to receive pilot commands, sense aircraft states, generate flight control commands, and perform data communication. Due to the real-time computing requirements, the limited space and the weight capacity of the model, trade-offs must be made when designing the layout and determining the components of the flight control system[23,24]. The resulting overview of the avionic system is depicted in Fig 5. Only the instrumentations for measurement of flight variables and deflection of control surfaces will be carried on-board. The aircraft model is connected to the ground facility via an 'umbilical' cord which provides electrical power and communication with the on-board payloads. The flight control computer is located aside the test section for a good pilot's view of the model motion.

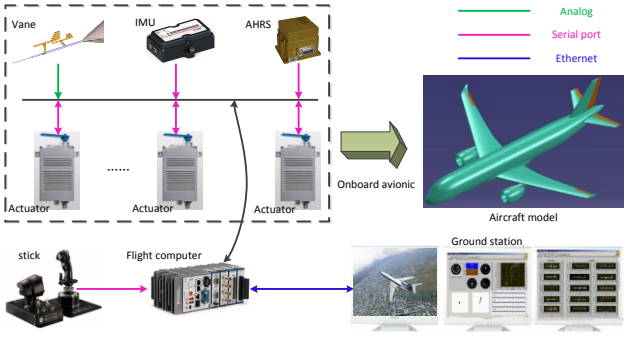

Fig. 5. Overview of the Avionic System

The external flight computer is able to renew the flight control law commands at frequencies higher than 200Hz for the fastest feedback rates, Onboard sensors are mainly used to measure the airflow angles(α, β), angular speed(p, q, r) and attitude(ψ, θ, φ). High bandwidth actuators are required by the dynamic scaling relationships to drive the surfaces. This places greater demands on some subsystems, such as the control period of flight computer, the bandwidth and the rate of actuator and sensor. Table 3 lists the primary avionic components used which are all COTS (Commercial-off-the-shelf) components and applicable for most civil and military aircrafts.

Table 3. Primary components for the avionic system

Component	Module	Specification
Flight computer	NI, cRIO9041	Real-time operating system, Reconfigurable FPGA, LabVIEW interface
Vane	SpaceAge, 100386	Output: α, β Range: ±60° Update rate:200 Hz Interface: voltage Physical: 38×84×13mm, 15g
IMU	Sensonor, STIM202	Output: p, q, r Range: ±400°/sec Update rate:262 Hz Interface:RS422 Physical: 45×39×20mm, 55g
AHRS	Memsic, AHRS 440	Output: ψ, θ, φ Range: ±180° Accuracy: < 3° (ψ), <1.5° (θ, φ) Update rate:100Hz Interface:RS232 Physical: 76×95×76mm, 580g
Actuator	CARDC, electro mechanical actuators	Torque: 120 Ncm Speed: 250°/s Update rate: 200Hz Interface:RS485 Physical: 42×66×22mm, 132g
Pilot stick	BGsystem, JF3	Output: roll, pitch and twist interface: voltage

To avoid building one flight computer system for each aircraft model, the RCP technique is employed as the framework of the flight control system (FCS), as shown in Fig 6. The RCP based framework can be used to explore flight computer systems for different aircraft models without any significant hardware or software modifications[25]. The host computer is a workstation, which provides MATLAB and Simulink environments for control law design and simulation, allows debugging, manipulating and monitoring the flight test process. The target computer is a controller called CompactRIO from NI. The CompactRIO runs a real-time operating system which executes compiled LabVIEW diagrams and has FPGA resources which provide the implementation of drivers for actuators and sensors. The only drawback is that the code of the flight control law should be rewritten by hand in LabVIEW

according to the Simulink diagrams. However, this framework overcomes the tradeoff between cost and efficiency of flight control system integration.

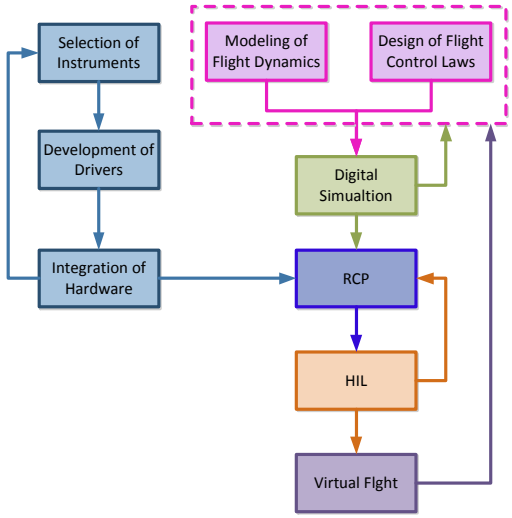

Fig. 6. RCP Based Workflow for Integration of FCS

2.4 Flight Control Law

Flight control law (FCL) is required to allow the augmented aircraft model to be manipulated in 3 rotational DOF at a variety of speeds and angle of attack. To obtain flight control laws that are applicable to the full scale aircraft, the nonlinear flight dynamics model and control law gains must be also scaled as summarized in Table 4.

Table 4. Dynamic scaling parameters for FCL

Parameter	Scale factor
Bandwidth and rate of actuator	$N^{-0.5}$
Bandwidth of sensors	$N^{-0.5}$
Bandwidth of filter	$N^{-0.5}$
Frequency of dynamic element	$N^{-0.5}$
Feedback gain of angular rate	$N^{0.5}$
Feedback gain of angular acceleration	N

In the VFT setup, the aircraft model is held at its CG by the 3-DOF rig, thereby eliminating all the three translational freedoms. As a result, there is no need to simulate the scaled engine for majority cases. Besides, the normal load factor is unavailable from the onboard sensors. It means that implementation and validation of normal-load-factor control augmentation system (CAS) for longitudinal FCL is infeasible in the VFT. The top-level FCL scheme is depicted in Fig 7. There are 2 mutually exclusive modes for FCLs: baseline and research.

Baseline FCL is a conventional controller intended to stabilize the aircraft, improve the flying and handling quality, and provide a baseline for comparison of advanced research control laws.

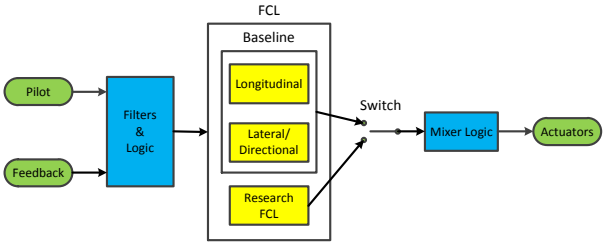

Fig. 7. Top-level Flight Control Law Scheme

Baseline control laws are developed using linear decoupled state-space models at different trimming points via classical or modern control techniques, such as root locus, eigenstructure assignment, LQR and dynamic inversion, etc.[26]. For conventional flight cases, the research FCLs are controllers designed for performance improvement with advanced control techniques, such as robust control, adaptive control, artificial intelligence control, etc. For challenging flight cases, research FCLs are controllers designed for extended flight envelop, including thrust vectoring control, self-repairing control, and post-stall maneuver, etc.

Fig. 8. Top-level Flight Control Law Scheme

2.5 Ground Control Station

The ground control station (GCS) is used to configure the testing setup parameters, monitor the flight state, visualize the flight condition and record the data for post-test analysis. It consists of a desktop computer running the GCS software connected to a flight control computer and a visualization computer via UDP Ethernet. The GCS software interface, as shown Fig 8, is

designed to present the critical flight states in real time with curves and visual indicators, including airflow angle, angular speed, pilot command and surface deflection, etc. With the help of this interface, the research pilot is able to engage and disengage FCS functions, to handle the aircraft configurations and to tune the FCL parameters during the tests.

3 Typical Application and Results

To demonstrate the facility capabilities, a series of simulations and virtual flight tests involving a 1/10 scale model was carried out at LSAI, as shown in Fig 9.

(a) Overview of Virtual Flight Test

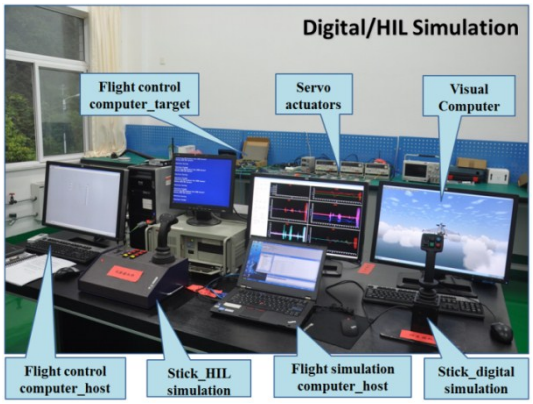

(b) Overview of Simulations

Fig. 9. Simulation and Virtual Flight Research of an Aircraft

3.1 Digital Simulation

The digital simulation allows to test the correctness of designed nonlinear aircraft model and control laws within the Matlab/Simulink environment on a desktop computer, as in Fig 10.

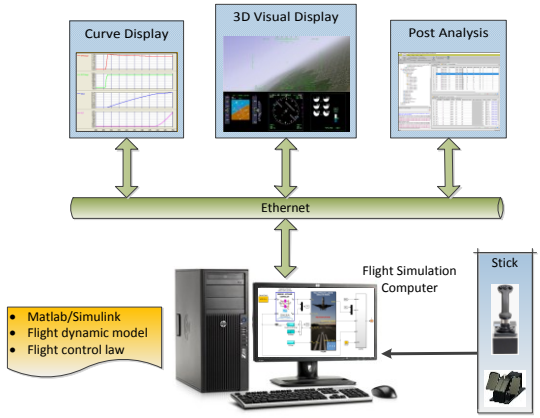

Fig.10 Digital simulation setup

The flight control laws for the 1/10 scale model are developed to provide good flying qualifies. There are two control law options in the longitudinal channel, as shown in Fig 11. Transfers between the pitch-rate CAS and angle-of-attack CAS are controller by the 'Threshold' and 'Switch' blocks. The pitch-rate CAS utilizes the pitch stick position to command a pitch rate, and with no pitch stick input, the model control laws would attempt to maintain the current pitch attitude. The angle-of-attack CAS combines the threshold, the alpha and the pilot command through an integrator, but removes the pitch rate integrator channel. Additional proportional feedback of alpha and pitch rate is added after the integrator. With centered stick, it was essentially a pitch attitude hold system. The model control laws would attempt to maintain the angle of attack at the threshold. Besides, the lateral channel utilizes a roll-rate CAS, the directional channel uses a sideslip CAS. The lateral/directional control laws include an aileron-to-rudder interconnect (ARI) so that one pilot could fly the roll-yaw axes of the aircraft model with one control.

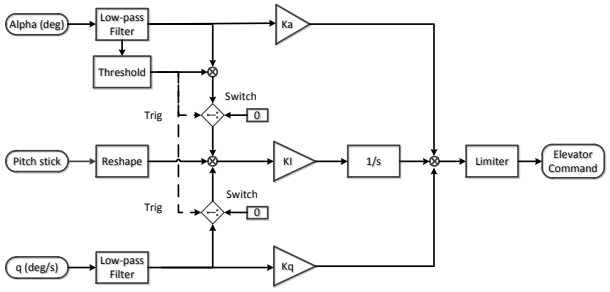

Fig. 11. Block diagram for longitudinal FCL

Fig 12 shows the square response of longitudinal channel. The square input is zero

first, positive for 0.5 s, and then zero. The settling time of the pitch rate step response is about 0.15 s, alpha increases continuously to about 14.8°. When the pilot input becomes zero, the pitch rate decreases rapidly to zero with a little overshoot. However, alpha almost holds its value. Results from the digital simulations indicate that the longitudinal channel of the closed loop system acts as a rate command and attitude hold system, which is a correctness validation for the pitch-rate CAS of longitudinal FCL.

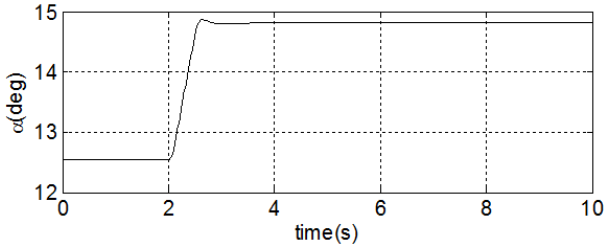

(a) Alpha

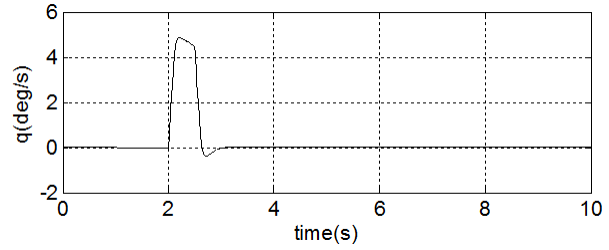

(b) Pitch rate

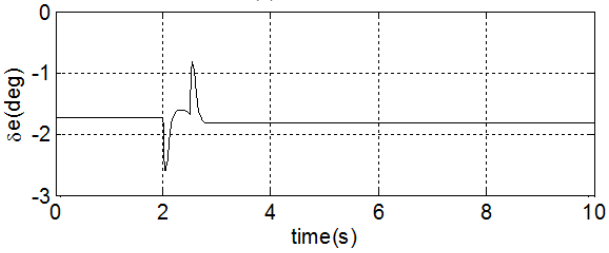

(c) Elevator

Fig.12 Response of pitch angle/rate command

3.2 Hardware-In-the-Loop Simulation

The hardware-in-the-loop (HIL) simulation allows to test implemented FCL codes running on the flight computer, as shown in Fig 13. The differences between HIL and digital simulation include:

- Matlab/Simulink blocks of the nonlinear aircraft model are compiled to C codes by Tornado and distributed to the flight simulation computer, which can run it in real time by the Vxworks operating system.
- The FCL blocks are rewritten by hand with LabVIEW in the flight control computer and then transferred to C codes in real time operating system or FPGA circuits with the CompactRIO benchmark.
- The flight simulation computer communicates with the flight control computer in real time via the UDP Ethernet.

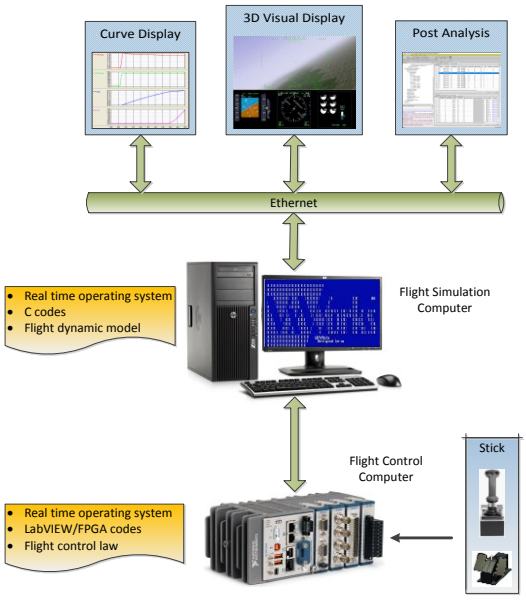

Fig.13 Hardware-in-the-loop simulation setup

Fig 14 compares the longitudinal response of the digital simulation with the HIL simulation response. The pilot square input scenario is first zero, moderate positive, small negative, again zero, moderate positive, and then zero. The responses of alpha, pitch rate and elevator for the two simulation cases agree well with each other. This means that the FCLs are implemented in the flight control computer correctly and that the real time computing capabilities of the flight control computer are sufficient.

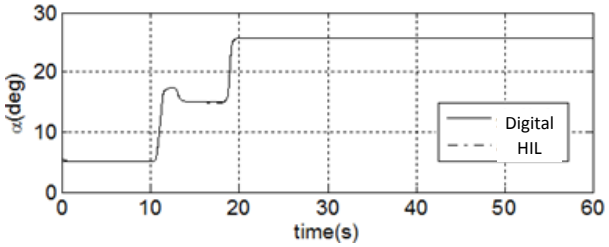

(a) Alpha

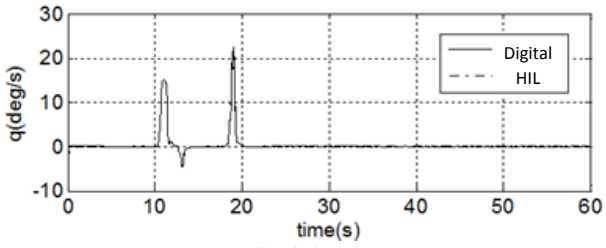

(b) Pitch rate

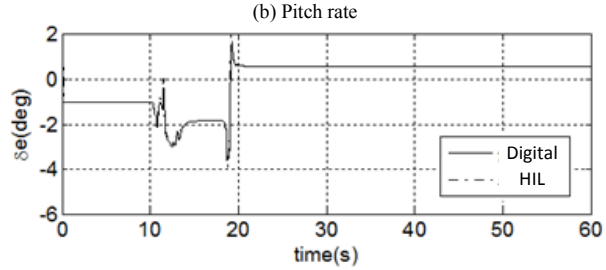

(c) Elevator

Fig.14 Comparison between digital and HIL simulation

3.3 Virtual Flight Test

The VFT is a 3-DOF dynamic flight environment for validation and evaluation of an aircraft's stability, controllability and flying quality, as depicted in Fig 15. Here, the nonlinear aircraft model used in the HIL simulation is substituted with the combination of wind tunnel flow field, scaled aircraft model, 3-DOF rig, and onboard avionics to provide an physical simulation that closely replicates the attitude motions of the full-scale aircraft. As a result, the VFT is particularly useful in challenging flight regimes that are dynamic or difficult to model such as stall and departure at high angle of attack, fault conditions and configuration transitions, etc.

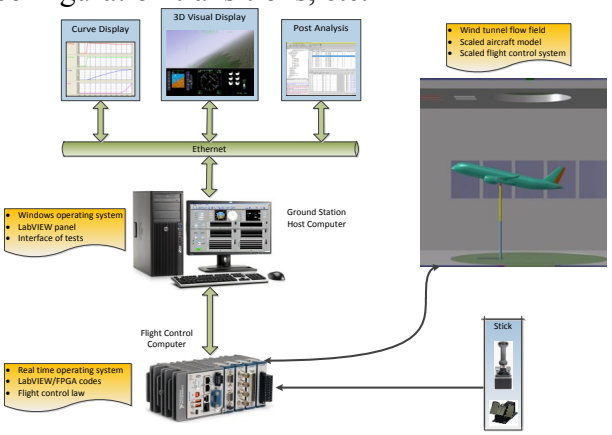

Fig.15 Construction of the virtual flight system in wind tunnel

For the 1/10 scaled aircraft model, the FCLs over a large range of alpha, including the threshold trigged structure modification are tested and presented in Fig 16. The scenario of test is: switch on the FCL in flight control computer; speed up the wind speed in wind tunnel and keep it steady at 30 m/s; manipulate the motion of aircraft model to 1g wing level at about 9° alpha; and then conduct the following manipulation scenario: Firstly, pull the stick back to the minimum position, the aircraft model noses up rapidly, the peak pitch rate reaches 48°/s, alpha steps to about 23.5° with some overshoot and oscillation; Secondly, drop the stick to the neutral position, the aircraft model noses down to the positive threshold (alpha=13°) with a peak pitch rate of -38°/s; Then, push the stick to the maximum position, the aircraft model nose down (-18°/s at the peak) further to and oscillate with a small amplitude around alpha= -8°. At last, drop the stick to the neutral position again, the aircraft model noses up to and maintains at the negative threshold (alpha= -5°). By comparison, one can note that the longitudinal responses of aircraft model in VFT are well consistent with the responses in digital simulation under the same manipulation scenario. However, due to the limited bandwidth of actuators and sensors, there are more overshoot and oscillation of alpha, and some delay of pitch rate in VFT; due to the geometry error of the aircraft model structure and assembling error of control surfaces, there is some translation of elevator deflection in VFT.

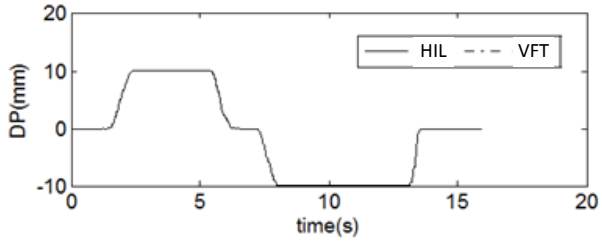

(a) Longitudinal pilot command

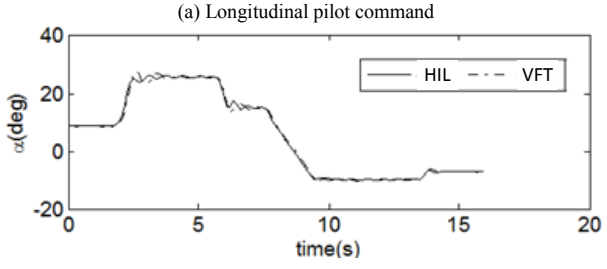

(b) Alpha

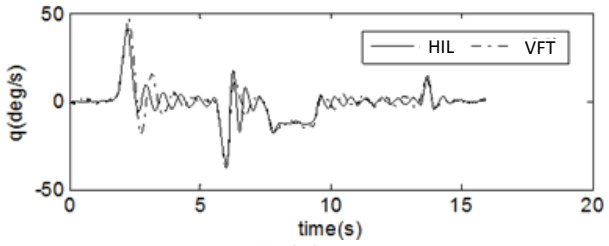

(c) Pitch rate

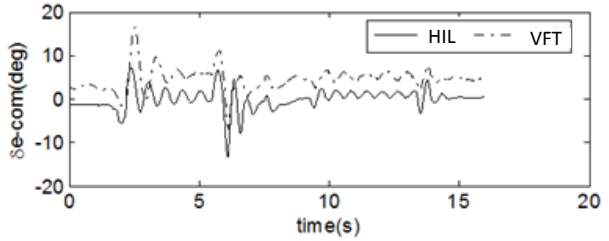

(d) Elevator

Fig.16 Comparison between HIL simulation and virtual flight test of an aircraft

4 Conclusions

A VFT facility has been developed to perform realistic simulation of attitude motion with dynamically scaled aircraft model and flight control system. The 3-DOG rig uses a CTOS spherical rolling joint to eliminate the translational DOFs and allow the rotational DOFs with respect to the CG of aircraft model. This rig offers advantages for simplicity and low friction. A quantitative test and an analysis of the friction induced damping of the aircraft model have been conducted for proof. A dynamic scaling criterion for aircraft model and avionic system design and integration is presented with additions to account for weight and size constraints. A RCP based generic FCS development framework applicable for a variety of aircrafts is introduced so that the designers can get much relief form hardware integration and concentrate more on the FCL implementation. Since the majority of components used in the facility is COTS available and complies with most of the aircrafts, it is flexible, efficient, and low cost to implement, validate and evaluate FCLs based on this VFT facility.

To illustrate the capabilities of the facility, digital simulations, HIL simulations and VFT tests are conducted for a 1/10 scaled aircraft model. Correctness of FCLs and real time capabilities of the flight control computer are tested and verified by simulations. Conventional maneuvers over large range of angle alpha are conducted to demonstrate the functions and performances of the longitudinal FCL by VFT tests. With this facility, it is potential to evaluate the handling and flying quality, and to identify the dynamic models of aircraft models in the future.

References

[1] J. Pattinson, M. H. Lowenberg, and M. G. Goman. A Multi-Degree-of-Freedom Wind Tunnel Manoeuvre Rig for Dynamic Simulation and Aerodynamic Model Identification, *Journal of Aircraft, Vol. 50, No. 2, March-April 2013*.

[2] Q. Wang, W.Q. Qian, K.F. He. Unsteady aerodynamic modeling at high angles of attack using support vector machines. Chin J Aeronaut, 28 (3) (2015), pp. 659-668

[3] J.-M. Biannic, L. Burlion, H. de Plinval. Robust control design over large flight envelopes: A promising approach for aerial robotics. In a special issue of the AerospaceLab journal on Aerial Robotics. Issue 8, December 2014.

[4] Abramov, N. et al. (2014) Flight Envelope Expansion via Active Control Solutions for a Generic Tailless Aircraft. 29th ICAS Congress 2014. St. Petersburg, Russia

[5] Araujo-Estrada, S.A., Lowenberg, M.H., Neild, S. and Goman, M. (2015) Evaluation of Aircraft Model Upset Behaviour Using Wind Tunnel Manoeuvre Rig. AIAA Atmospheric Flight Mechanics Conference, AIAA SciTech, (AIAA 2015-0750).

[6] Yuji M, Takeharu K, Masahiko S. Evaluation of self-repairing flight control system by wind-tunnel free-flight dynamic test. 24th congress of the international council of the aeronautical science; 2004.

[7] Abramov, N. et al. (2014) Flight Envelope Expansion via Active Control Solutions for a Generic Tailless Aircraft. 29th ICAS Congress 2014. St. Petersburg, Russia

[8] Bruce D O, Brandon J M, et all. Overview of dynamic test techniques for flight dynamics research at NASA LaRC (Invited)[R]. NASA Langley Research Center, 2006.

[9] M. Huang, Z.W. Wang. A review of wind tunnel based virtual flight testing techniques for evaluation of flight control systems. Int J Aerospace Eng, 2015 (1) (2015), pp. 1-22

[10] Lawrence FC, Mills BH. Status update of the AEDC virtual flight testing development program. Reston: AIAA; 2002. Report No.: AIAA-2002-0168.

[11] D.I. Ignatyev, K.G. Zaripov, M.E.Sidoryuk, K.A. Kolinko, A.N. Khrabrov. Wind Tunnel Tests for Validation of Control Algorithms at High Angles of

Attack Using Autonomous Aircraft Model Mounted in 3DOF Gimbals. AIAA Atmospheric Flight Mechanics Conference, AIAA Aviation, Washington, D.C., USA, AIAA 2016-3106, 2016.

[12] Gatto A, Lowenberg M.H. Evaluation of a three degree-of-freedom test rig for stability derivative estimation. J. of Aircraft. V. 43, N. 6, pp 1747-1762, 2006.

[13] Cook, M., "On the Use of Small Scale Aircraft Models for Dynamic Wind Tunnel Investigation of Stability and Control," Transactions of the Institute of Measurement and Control, Vol. 9, No. 4, 1987, pp. 190–197.

[14] Araujo-Estrada, S.A. et al. (2015) Wind Tunnel Manoeuvre Rig: A Multi-DOF Test Platform for Model Aircraft. 54th AIAA Aerospace Sciences Meeting, AIAA SciTech, (AIAA 2016-2119).

[15] Jay M B, James M S, et all. Free-flight investigation of fore-body blowing for stability and control[R]. AIAA-96-3444,1996

[16] Jackson E B, Buttrill C W. Control laws for a wind tunnel free-flight study of a blended-wing-body Aircraft[R]. NASA/TM,2006.

[17] Chambers J R. Modeling flight: the role of dynamically scaled free-flight models in support of NASA's aerospace programs [R], NASA SP 2009-575.

[18] Cen, F., Li, Q., Fan, L., Liu, Z., Sun, H.: Development of a pilot-in-loop real-time simulation platform for wind tunnel free-flight test. In: IEEE International Conference on Information and Automation, pp. 2433–2438. IEEE, August 2015

[19] Guo Linliang,Zhu Minghong,Nie Bowen. Initial virtual flight test for a dynamically similar aircraft model with control augmentation system [J]. Chinese Journal of Aeronautics, 2017, 30(2): 602-610.

[20] B. Nie, L. Guo, P. Kong, M. Jiang and M. Zhu, "Hardware development of the wind tunnel based virtual flight system," Proceedings of 2014 IEEE Chinese Guidance, Navigation and Control Conference, Yantai, 2014, pp. 1135-1138.

[21] Gatto A. Application of a Pendulum Support Test Rig for Aircraft Stability Derivative Estimation[J]. Journal of Aircraft, 2006, 46(3): 927-934.

[22] Wolowicz, C., Bowman Jr, J., and Gilbert, W., 1979. Similitude requirements and scaling relationships as applied to model testing. NASA technical Paper, 1435.

[23] Bruce Owens, David Cox, and Eugene Morelli., Development of a Low-Cost Sub-Scale Aircraft for Flight Research: The FASER Project. 25th AIAA Aerodynamic Measurement Technology and Ground Testing Conference. San Francisco, California.

[24] Austin Murch. "A Flight Control System Architecture for the NASA AirSTAR Flight Test Infrastructure", AIAA Guidance, Navigation and Control Conference and Exhibit, Guidance, Navigation, and Control and Co-located Conferences.

[25] LIU Z T, NIE B W, GUO L L, et al. Rapid prototyping and implementation of flight control system for wind tunnel virtual flight test[J]. Acta Aerodynamica Sinica, 2017, 35(5): 700-707.

[26] Stevens, B.L., Lewis, F.L., and Johnson, E.N., Aircraft Control and Simulation: Dynamics, Controls Design, and Autonomous Systems, 3rd Edition, Wiley, 2015.

5 Contact Author Email Address

mailto:xuanwen1981@163.com

Copyright Statement